Journal of Turbulence
Vol. 13, No. 13, 2012, 1–26

Taylor & Francis
Taylor & Francis Group

Characterizing and mitigating the wind resource-based uncertainty in farm performance

Achille Messac[a]*, Souma Chowdhury[b], and Jie Zhang[b]

[a]*Department of Mechanical and Aerospace Engineering, Syracuse University, Syracuse, NY;*
[b]*Department of Mechanical, Aerospace, and Nuclear Engineering, Rensselaer Polytechnic Institute, Troy, NY*

(*Received 29 September 2011; final version received 18 January 2012*)

A farm planning strategy that simultaneously accounts for the key engineering design factors and addresses the uncertainties in a wind project can offer a powerful impetus to the development of wind energy. In this context, the resource itself is highly uncertain – wind conditions, including *wind speed*, *wind direction*, and *air density*, show strong temporal variations; in addition, the distribution of wind conditions varies significantly from year to year. The resulting ill-predictability of the annual distribution of wind conditions introduces significant uncertainties in the *estimated resource potential* or the *predicted performance* of the wind farm. In this paper, a new methodology is developed (i) to characterize the uncertainties in the annual distribution of wind conditions, and (ii) to model the propagation of uncertainties into the local wind power density (WPD) and into farm performance evaluation. Key measures of farm performance include annual energy production (AEP), cost of energy (COE), and payback period. Both parametric and nonparametric uncertainty models are formulated, which can be leveraged in conjunction with a wide variety of stochastic wind distribution models. The AEP and the COE are evaluated using advanced analytical models, adopted from the recently developed Unrestricted Wind Farm Layout Optimization (UWFLO) framework. The year-to-year variations in the wind distribution and the quantified uncertainties are illustrated using two case studies: an onshore and an offshore wind site. Appreciable uncertainties are observed in the estimated yearly WPDs over the 10-year period – approximately 11% for the onshore site and 30% for the offshore site. The uncertainty in COE is mitigated for the onshore site using the nonparametric uncertainty model *within* the UWFLO framework. The ensuing robust optimization process illustrated how important it is to reduce the sensitivity of the farm performance to unreliable wind conditions, even though they may be frequent in certain years and/or contain higher energy density.

Keywords: annual energy production; cost of energy; farm layout optimization; uncertainty; wind distribution

1. Introduction

1.1. *An overview of wind farm planning*

Renewable energy resources, particularly wind energy, have become a primary focus in government policies, in academic research, and in the power industry. The practical viability of energy production is generally governed by such factors as (i) the potential for *large-scale energy production*, (ii) the predictability of the power to be supplied to the grid,

*Corresponding author. Email: messac@syr.edu

ISSN: 1468-5248 online only

http://dx.doi.org/10.1080/14685248.2012.661863
http://www.tandfonline.com

and (iii) the expected *return on investment*. The various uncertainties in wind energy impact the reliable determination of these viability factors. The 2010 worldwide nameplate capacity of wind-powered generators was approximately 2.5% of the worldwide electricity consumption [1]; and the annual growth rate of wind power in 2010 was the lowest since the year 2004 [1]. For wind to play a more prominent role in the future energy market, we need steady improvement in the wind power generation technology; such advancement can be realized in part through appropriate quantification of the various uncertainties and explicit consideration of their influences in the optimal design of wind farms.

The primary objectives of *robust and optimal wind farm planning* should include:

- **Objective 1:** optimal selection of a site based on the quality of the local wind resource,
- **Objective 2:** maximization of the annual energy production (AEP) and/or minimization of the cost of energy (COE) of the farm, and
- **Objective 3:** maximization of the reliability of the predicted energy production.

One of the major activities in site selection is to determine the wind resource potential at the candidate site, a popular measure of which is the estimated local wind power density (WPD). Another important activity in this context is to determine the levels of turbulence and the resulting wind loads at the concerned site. This activity promotes better decision-making when selecting wind turbines for the site and also helps in predicting the life cycle cost of developing a wind farm at that site – higher wind loads generally indicate higher costs. Other site selection criteria include, but not limited to, (i) local topography, (ii) vegetation, (iii) distance to major grid connections, (iv) ease of land acquisition, and (v) site accessibility for turbine transport and maintenance.

Post site selection, Objective 2 can be accomplished through effective planning of the following engineering factors:

(1) The nameplate capacity (installed capacity) of the wind farm,
(2) The farm land configuration (including land area, land shape and N-S-E-W orientation),
(3) The layout of the wind farm, and
(4) The type(s) of wind turbines to be installed in the wind farm.

The power generated by a wind farm is a variable quantity that is a function of a series of environmental and engineering parameters. Several of these parameters are highly uncertain, e.g., wind conditions at the site, power performances of individual turbines, and occurrence of extreme weather conditions. A careful characterization of these uncertainties and the modeling of their propagation into the overall system should provide a credible quantification of the long-term wind farm energy production. The subsequent mitigation of these uncertainties during the optimal wind farm design stage would accomplish Objective 3. At the same time, regarding site selection, it is generally considered that a desirable wind resource is one that has *stable high speeds* [2]. *Stable high speeds* refer to the availability of overall higher energy density (higher averaged wind speed) along with low fluctuations. Fluctuations in the short time scale are caused by atmospheric turbulence, the discussion of which is however not within the scope of this paper. In the meantime, there are two sources of long-term fluctuations [3]: (i) *the annual variation in wind conditions* (over the year), which can be estimated through wind distribution modeling, and (ii) *the variation in the annual wind distribution from year to year*, which can be characterized using the uncertainty models presented in this paper.

1.2. *Wind farm performance*

Two primary measures of wind farm performance are the *annual energy production* (AEP) capacity and the *cost of energy* (COE) for the farm. Another economic parameter, the *payback period*, represents how financially attractive it is to build a wind farm of a certain capacity at a particular site. *Payback period* can be more precisely defined as the period of time (in years) required by the return on investment (in the farm) to repay the original farm costs incurred. Considering the variation in wind speed and wind direction, the expected AEP is estimated by the aggregate farm power generation over the annual wind distribution. For any given wind condition, the total power extracted by a wind farm is significantly less than the simple summation of the power extracted by each turbine when operating as stand-alone entities [4]. This deficiency can be attributed to the loss in the availability of energy due to *wake effects*, which is the shading effect of a wind turbine on downstream turbines. Energy deficit due to mutual shading effects can be determined using wake models that provide a measure of the growth of the wake and the velocity deficit in the wake with distance downstream from the wind turbine. Standard analytical wake models include the Park wake model [5, 6], the modified Park wake model, and the eddy viscosity wake model. The reduction in the wind farm efficiency caused by wake effects depends primarily on the geometric arrangement of wind turbines in the farm (farm layout) and on the expected distribution of wind conditions at the concerned site.

To address this energy deficiency, several wind farm layout modeling approaches have been reported in the literature: (i) models that assume an array-like (row-column) farm layout [4, 7], (ii) models that divide the wind farm into a discrete grid in order to search for the optimum grid locations of turbines [8, 9, 10, 11, 12], and (iii) models that consider the location coordinates of each turbine to be independent and continuous variables [13]. The recently developed Unrestricted Wind Farm Layout Optimization (UWFLO) method [13, 14] avoids limiting assumptions presented by other methods pertaining to the layout pattern and the selection of turbines. In this paper, we adopt the power generation model from the UWFLO method [14] to evaluate the AEP. This power generation model implements a standard analytical wake model [15] to account for the wake losses. The UWFLO power generation model was validated by Chowdhury et al. [13] using experimental data reported by Cal et al. [16]. An advancement of the UWFLO method is developed in this paper in order to perform *robust wind farm optimization* – mitigation of the uncertainties in long-term farm performance.

Numerous techniques have been developed to evaluate the cost of onshore and offshore wind farms in the last 20 years. Notable examples include: short-cut model [17], cost analysis model for the Greek market [18], OWECOP-Prob cost model [19], JEDI-wind cost model [20], and the Opti-OWECS cost model [21]. In this paper, we implement the *Response Surface-based Wind Farm Cost* (RS-WFC) model reported by Chowdhury et al. [14]. Such a cost model has two major advantages: (i) the cost is represented by a continuous analytical function that can be easily used as a criterion function in optimization irrespective of the search strategy, and (ii) the estimated cost function is highly adaptive to the local cost data provided for training the model.

1.3. *Uncertainties in a wind farm*

The physical uncertainties affecting the performance of a wind farm are primarily of two types:

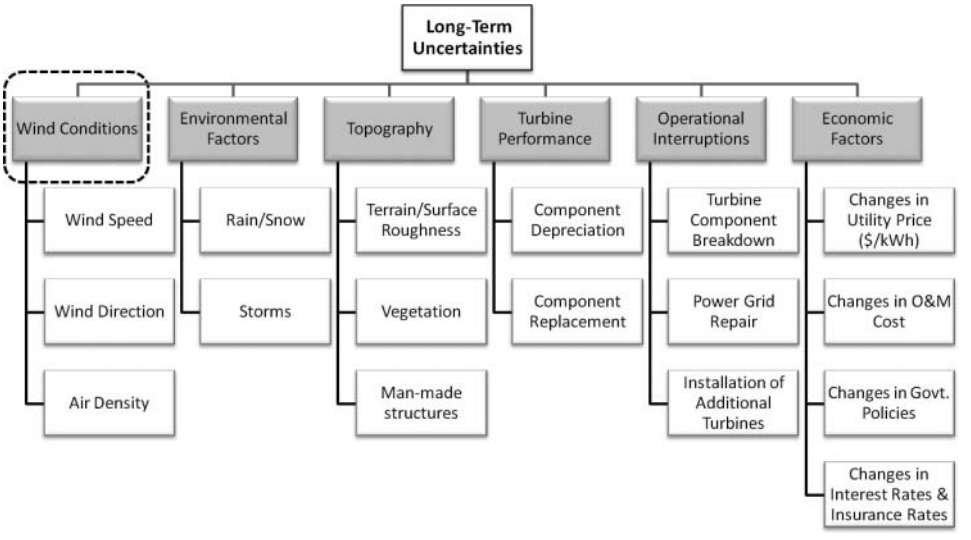

Figure 1. Classification of the long-term uncertainties in wind energy.

(1) Short-term uncertainties: uncertainties introduced by boundary layer turbulence and by other flow variations that occur in a small time scale (of the order of minutes), as well as by short-lived extreme weather conditions; and
(2) Long-term uncertainties: uncertainties introduced by the long-term variations in wind conditions and by other environmental, operational and financial factors.

The physical sources of long-term uncertainties can be further broadly classified into the categories shown in Figure 1. In this paper, the category that is highlighted by the encircling dashed rectangle in Figure 1 is specifically addressed. The incoming wind condition, comprising wind speed, wind direction, and air density, is a major factor that regulates the power generated by a wind farm. Owing to seasonal effects, these conditions vary significantly over the course of a year. The overall trend of the annual distribution of wind conditions is however expected to remain fairly similar over years. In the literature, the long-term variation in wind conditions has been represented by several parametric [23, 32] and nonparametric distribution models [24]. The predicted wind distributions themselves have been observed to be appreciably uncertain, as is evident from their year-to-year variations, which is illustrated in Section 2.2.

From an optimization standpoint, a reliable wind farm design should be minimally sensitive to the uncertainties in the predicted wind distribution at the concerned site. For a given wind distribution, the AEP strongly depends on the following design factors: farm-land configuration, farm layout, and turbine selection. Chowdhury et al. [25] reported that robust optimization of these factors should seek to reduce the sensitivities of the AEP and/or the COE to the more uncertain wind conditions. In order to accomplish the reliability *objective*, it is necessary to accurately quantify the uncertainty in the farm performance, introduced by the ill-predictability of the local wind distribution. The quantification of this uncertainty and its subsequent mitigation are the primary contributions of this paper, which are accomplished through:

(1) A careful characterization of the uncertainties in the predicted long-term wind distribution,
(2) The modeling of the propagation of these uncertainties into the AEP and the COE, and
(3) The development and application of a robust wind farm optimization strategy that seeks to minimize the uncertainties without unreasonably compromising the farm performance.

Both parametric and nonparametric uncertainty models are developed in this paper, each with uniquely helpful attributes. The parametric uncertainty model can be applied in conjunction with standard parametric wind distribution models (e.g., Weibull and log-normal). The nonparametric uncertainty model can be applied in conjunction with both parametric and nonparametric wind distribution models. These uncertainty models address the variations in three major attributes of an incoming wind condition: wind speed, wind direction, and air density. However, for clearer illustration purposes, only wind speed and wind direction are considered in the case studies provided in this paper.

In this paper, progressive modifications are made to the UWFLO method, allowing the method to *minimize uncertainty in the farm COE*. This minimization is performed subject to an additional constraint that partially preserves the farm performance gain accomplished through *COE minimization*. The advanced UWFLO method thus presents a framework to design wind farms that are *reliably high-performing*. To the best of the authors' knowledge, such a robust optimal wind farm design strategy is unique in the literature. Section 2 presents and explores the wind distribution at two sample sites (onshore and offshore) to motivate the development of the wind uncertainty models. The resource potential and the farm performance models adopted from the UWFLO method are summarized in Section 3. The development and the application of the newly developed methods to characterize the uncertainties in wind conditions and to model the propagation of these uncertainties into the farm performance are presented in Section 4. The implementation of the new uncertainty quantification methods in the UWFLO framework to perform robust optimization of the wind farm is presented in Section 5.

2. Ill-predictability of the wind distribution

2.1. *Estimation of local wind distribution*

As briefly discussed in the previous section, the state of the art in wind distribution estimation introduces significant uncertainties in wind resource assessment. Two sample sites are used to explore this issue and illustrate the development of the uncertainty models. These sites are: (1) an onshore site at the Baker wind station in North Dakota, and (2) an offshore site at the wind station Station 44013-BOSTON, 16 NM East of Boston, off the coast of Massachusetts. The wind data for the onshore wind farm is obtained from the North Dakota Agricultural Weather Network (NDAWN) [26], and that for the offshore wind farm is obtained from the National Data Buoy Center (NDBC) [27]. In both cases, we consider the daily averaged recorded data over a span of 10 years, from January 2000 to December 2009. Pertinent details of the Baker station and Station 44013 are provided in Table 1. The recorded annual distributions of wind speed and wind direction at the two stations are illustrated by Windrose diagrams in Figures 2(a) and 2(b). In the Windrose diagrams, each of the 16 sectors represents the respective probability of wind blowing from that direction.

One of the most widely used model for characterizing the annual variation in wind speed is the two-parameter Weibull distribution [28, 22]. Other models used to characterize this variation include the one-parameter Rayleigh distribution, the three-parameter generalized

Table 1. Details of the two wind stations.

Parameter	Onshore station [26]	Offshore station [27]
Location	Baker, ND	Station 44013, MA
Latitude	48.167°N	42.346°N
Longitude	99.648°W	70.651°W
Elevation	512 m	Sea level
Measurement height	3 m above site elevation	5 m above site elevation
Water depth	NA	61 m

gamma distribution, the two-parameter log-normal distribution, the three-parameter beta distribution, the bimodal Weibull model, the two-parameter inverse Gaussian distribution, the singly truncated normal Weibull mixture distribution, and the maximum entropy probability density function (pdf) [22, 23]. The majority of these wind distribution models make limiting assumptions regarding the correlativity and the modality of the variations in wind speed and wind direction.

In more recent publications, a limited number of methods have been proposed to capture the joint annual variation of wind speed and wind direction [22, 29, 30, 32]. However, these methods do not explicitly account for the variation in air density; Zhang et al. [24] have shown that the air density at a site in North Dakota can vary up to 30% over the year. In this paper, we use the Multivariate and Multimodal Wind Distribution (MMWD) model developed by Zhang et al. [24] for both univariate and multivariate wind distributions. The MMWD model can capture the joint variation of wind speed, wind direction, and air density, and also allows representation of multimodally distributed data. For the onshore and offshore sites considered in this paper, the MMWD model provides the most accurate representation of the recorded wind data [24].

Multivariate kernel density estimation (KDE) method [33] is used to develop the MMWD model. KDE is a nonparametric method for estimating the pdf of random variables. For a $d - variate$ random sample $U_1, U_2, \ldots, U_n$ drawn from a density f, the multivariate

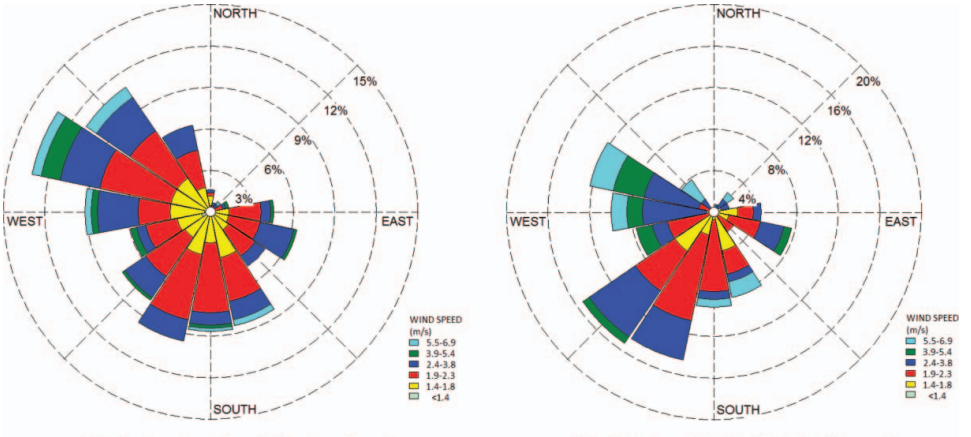

(a) Baker station, ND (onshore) (b) Station 44013, MA (offshore)

Figure 2. Wind rose diagrams: recorded wind data from 2000 to 2009.

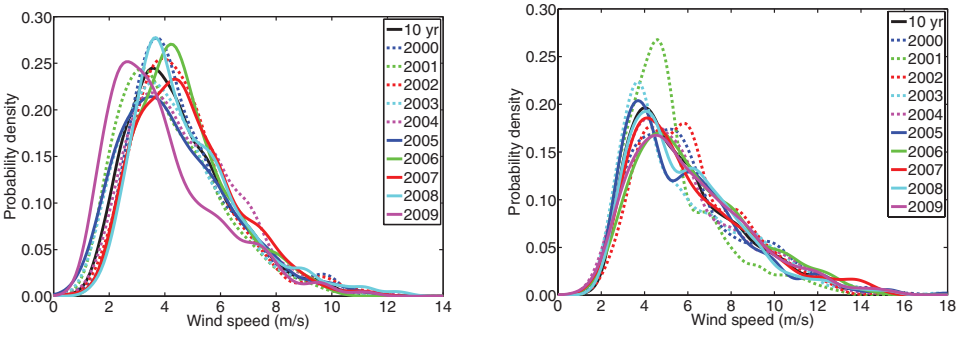

(a) Baker station, ND (onshore) (b) Station 44013, MA (offshore)

Figure 3. Annual and 10-year distributions of wind speed (2000–2009) estimated by the MMWD model.

KDE is defined to be

$$\hat{f}(u;H) = n^{-1}\sum_{i=1}^{n} K_H(u - U_i), \tag{1}$$

where $u = (u_1, u_2, \ldots, u_d)^T$ and $U_i = (U_{i1}, U_{i2}, \ldots, U_{id})^T$, $i = 1, 2, \ldots, n$. In this equation, the kernel $K(u)$ is a symmetric pdf, H is the bandwidth matrix that is symmetric and positive-definite, and $K_H(u) = |H|^{-1/2}K(H^{-1/2}u)$. The choice of K is generally not crucial to the accuracy of kernel density estimators [34]. In this paper, we consider $K(u) = (2\pi)^{-d/2}\exp(-\frac{1}{2}u^T u)$. In contrast, the choice of the bandwidth matrix H is crucial in determining the performance of $\hat{f}$ [35]. In the MMWD model, an optimality criterion, the asymptotic mean integrated squared error [35], is used to select the bandwidth matrix.

2.2. *Illustrating the ill-predictability of the wind distribution*

For the sake of clarity in illustrating the year-to-year variations in wind distribution, we consider the univariate distribution of wind speed. Figures 3(a) and 3(b) show the wind speed distribution for each year within the period 2000–2009 at the onshore and offshore sites, respectively. Figures 4(a) and 4(b) show the estimated WPDs for the same period at the onshore and offshore sites, respectively. The determination of the WPD from the estimated wind distribution is detailed in Section 3.3.

Figures 3(a) and 3(b) show that the wind speed distributions at the onshore and offshore sites shift from year to year. Similarly, the WPD figures illustrate that the available energy at the onshore and offshore wind sites vary significantly from year to year. Most importantly, it is observed from these figures that the distribution of wind speed in a particular year could be significantly deviated from the overall 10-year distribution. Expectedly, over the 10-year period, the available wind energy at the offshore site is more stable than that at the onshore site, except for the year 2001. Overall, it is evident from these illustrations that – the wind distribution estimated from data recorded for a single year cannot *reliably* represent the long-term wind distribution at the concerned site. Commercial wind farms are designed for a lifetime of 15–25 years, and hence, require a reliable prediction of their

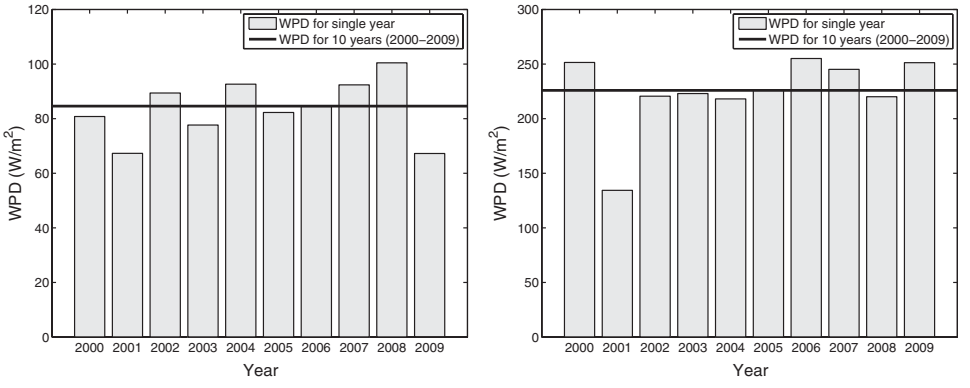

(a) Baker station, ND (onshore) (b) Station 44013, MA (offshore)

Figure 4. Annual and 10-year WPD (2000–2009) determined by the MMWD model [24].

expected performance over the lifetime. Such long-term prediction should account for the year-to-year variations in the wind resource.

To further explain this important uncertainty issue, we present illustrations of bivariate wind distributions for consecutive five-year periods: 2000–2004 and 2005–2009. Considering the year-to-year variations in the univariate wind speed distribution, the shifting is expected to be more pronounced in the case of the joint distribution of wind speed and wind direction. On the other hand, data recorded over a longer time period would be more representative of the likely future distribution of wind conditions. Figures 5(a) and 5(b) show the bivariate distributions of wind speed and wind direction at the onshore site for the periods 2000–2004 and 2005–2009, respectively. Figures 6(a) and 6(b) show the bivariate distributions of wind speed and wind direction at the offshore site for the periods 2000–2004 and 2005–2009, respectively. In the bivariate distribution plots, the wind direction axis in degrees represents the direction from which wind is flowing, measured clockwise with respect to the north direction; e.g., in the case of wind flowing from the east direction, $\theta = 90^\circ$. The same convention is used for all the graphical and numerical illustrations of

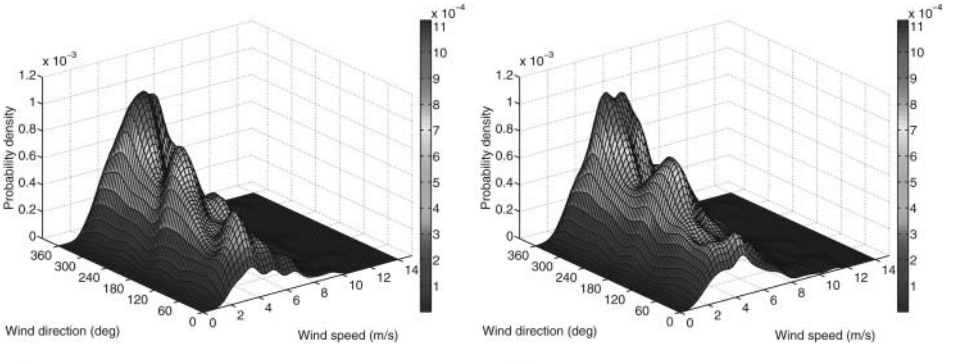

(a) For the period: Years 2000 - 2004 (b) For the period: Years 2005 - 2009

Figure 5. Five-year distribution of wind speed and wind direction at the onshore site (Baker Station, ND), estimated by the MMWD model.

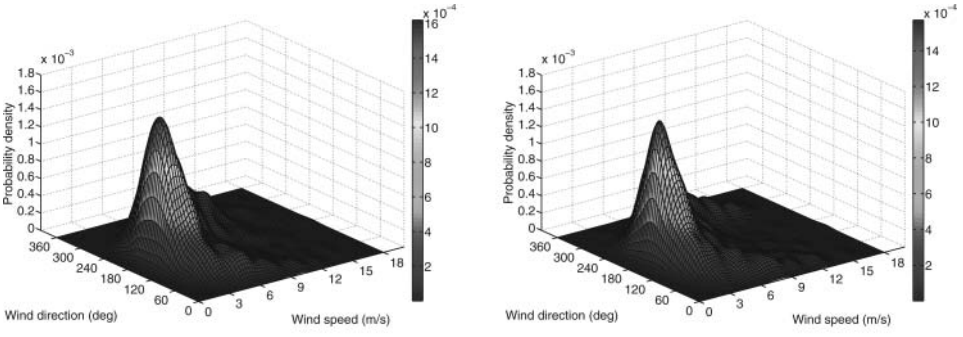

(a) For the period: Years 2000 - 2004 (b) For the period: Years 2005 - 2009

Figure 6. Five-year distribution of wind speed and wind direction at the offshore site (Station 44013, MA), estimated by the MMWD model.

wind direction in the remainder of the paper. Interestingly, it can be observed from Figures 5(a) and 5(b) that for the onshore site, the shifting between the consecutive five-year distributions is somewhat smaller than the year-to-year variations. The shifting in the consecutive five-year distributions in the case of the offshore site (Figures 6(a) and 6(b)) is even smaller than that for the onshore site. These observations indicate that *if the length of time of the recorded data (number of years) is (i) reasonably long and (ii) close to the succeeding length of time for which the prediction is being made, the estimated wind distribution is expected to be more reliable*. If either of the above criterion is not fulfilled, the predicted wind distribution is likely to be less reliable.

Owing to economic and timeline constraints in commercial wind farm development, wind measurements are generally recorded at potential sites for a period of perhaps one year. Measure-correlate-predict (MCP) methods are often used to correlate this 1-year on-site data to the concurring data at nearby meteorological station(s), and predict the approximate long-term wind distribution at the site [28, 3]. Nevertheless, in a practical scenario, the accuracy of long-term predictions obtained using MCP methods is subject to (i) the availability of a nearby meteorological station, (ii) the uncertainty associated with a specific correlation methodology [3], and (iii) the likely dependence of this correlation on physical features, such as the topography, the distance between the monitoring stations and the type of the local climate regime [36]. As a result, given the unavoidable practical constraints, the overall reliability of the predicted long-term wind distribution remains highly sensitive to the 1-year distribution of the recorded on-site data.

The uncertainty models proposed in this paper can therefore prove to be uniquely helpful in quantifying the uncertainty in the predictions made and can provide more credibility to the wind resource assessment and the farm performance estimation (during optimization). Where MCP methods are used, the uncertainty models developed in this paper could be directly applied to the long-term data recorded at the meteorological stations. Modeling the subsequent propagation of uncertainty through the MCP process would allow quantification of the expected uncertainty in the *on-site wind conditions*. In this context, an investigation of how the uncertainties explored in this paper interact with the *uncertainties inherent in the MCP correlation methodology* is also necessary. This investigation is an important topic for future research.

3. Modeling the resource potential and the farm performance measures

3.1. *Annual energy production (AEP) model*

The prediction of the AEP from a wind farm should account for the correlated long-term variations in wind speed, wind direction, and air density, which are together termed as "wind condition". To this end, the annual distribution of wind conditions is first represented using a suitable pdf, as discussed in Section 2.1. Subsequently, the AEP is determined by integrating the power generation function over the estimated annual wind distribution.

The AEP of a wind farm (in kWh), E_{farm}, at a particular location can therefore be expressed as:

$$E_{\text{farm}} = 365 \times 24 \int_{\rho_{\min}}^{\rho_{\max}} \int_{0^\circ}^{360^\circ} \int_{0}^{U_{\max}} P_{\text{farm}}(U, \theta, \rho)\ p(U, \theta, \rho)\, dU d\theta d\rho, \tag{2}$$

where $U^{\max}$ is the maximum wind speed at that location, $\rho_{\min}$ and $\rho^{\max}$ represent the minimum and the maximum air densities at the concerned location, respectively, and $p(U, \theta, \rho)$ represents the probability of occurrence of wind conditions defined by speed U, direction θ, and air density ρ. In Equation (2), $P_{\text{farm}}(U, \theta, \rho)$ represents the power generated by the farm for a wind speed U, a wind direction θ, and an air density ρ.

The net power generated by the farm, P_{farm}, is given by the summation of the power generated by the individual turbines, which is expressed as:

$$P_{\text{farm}} = \sum_{j=1}^{N} P_j, \tag{3}$$

where P_j represents the power generated by turbine j; and N represents the number of turbines in the farm. Subsequently, we express the overall farm efficiency, η_{farm}, as:

$$\eta_{\text{farm}} = \frac{P_{\text{farm}}}{\sum_{j=1}^{N} P_{0j}}, \tag{4}$$

where P_{0j} is the power generated by turbine j if operating as a stand-alone entity for the given incoming wind speed. The farm efficiency, η_{farm}, essentially represents the fraction of the available wind energy that is not lost to the wake effects. Based on the AEP given by Equation (2), the capacity factor (CF) of the farm can be expressed as:

$$\text{CF} = \frac{\text{AEP}}{365 \times 24 \times \sum_{j=1}^{N} P_{rj}}, \tag{5}$$

where P_{rj} is the rated power of turbine j. It is helpful to note that the accuracy of the analytical power generation model is significantly sensitive to that of the analytical wake models used. A discussion of the inherent assumptions in the analytical wake model and the detailed description of the power generation model can be found in the paper by Chowdhury et al. [13].

The power generated by a group of turbines in a wind farm is a complex function of the incoming wind attributes, the arrangement of turbines, and the turbine features; it is not a tractable analytical function that can be directly integrated. Hence, a numerical integration approach [37] is suitable for estimating the AEP, as given by Equation (2). To this end, the

Monte Carlo integration method is implemented using the Sobol's quasi-random sequence generator [38]. This class of integration methods is likely to provide greater accuracy for the same number of sample evaluations when compared with the repeated integrations using one-dimensional quadrature rule methods. The approximated total annual energy produced by the wind farm is expressed as:

$$E_{\text{farm}} = 365 \times 24 \sum_{i=1}^{n_p} P_{\text{farm}}(U^i, \theta^i, \rho^i)\, p(U^i, \theta^i, \rho^i) \Delta U \Delta\theta \Delta\rho, \quad \text{where}$$
$$\Delta U \Delta\theta \Delta\rho = (U_{\max} \times 360^\circ \times (\rho_{\max} - \rho_{\min}))/n_p, \tag{6}$$

and where n_p is the number of sample points used; the parameters U^i, θ^i, and ρ^i, respectively, represent the wind speed, the wind direction, and the air density of the incoming wind for the i^{th} sample point. Hence, the AEP is readily determined by the summation of the estimated power generation (P_{farm}) over the set of randomly distributed n_p wind conditions. In the remainder of the paper, the *predicted yearly probability of the i^{th} sample wind condition*, $p(U^i, \theta^i, \rho^i)$, is abbreviated as p_i.

3.2. *Wind farm cost model*

In the context of optimizing the farm layout and the turbine selection, the estimated annual cost of the farm can be represented as a function of *the number of turbines in the farm* and *the turbine rated powers* [14]. The annual farm cost is expressed in dollars per kW installed ($/kW). Radial basis functions are used to develop the Response Surface-based Wind Farm Cost (RS-WFC) model. In creating the response surface, the annual farm cost is expressed in dollars per kW installed ($/kW).

For a wind farm comprising N turbines, each with rated power P_r, the RS-WFC model cost, Cost(P_r, N), can be represented as:

$$\text{Cost}(P_r, N) = \sum_{i=1}^{n_p} \sigma_i \sqrt{\left(P_r - P_r^i\right)^2 + \left(N - N^i\right)^2 + c^2}, \tag{7}$$

where P_r^i and N^i, respectively, denote the turbine rated power and the number of turbines in a farm corresponding to the i^{th} training data. The value of the prescribed generic constant c is specified to be 0.9 in this paper, as recommended by Mullur and Messac [39]. The unknown coefficients (σ_i) are evaluated using the pseudo-inverse technique. In the case of a wind farm comprising multiple types of turbines, the cost function should be modified. To this end, the total annual cost in dollars ($) can be represented using a more generic expression, as given by:

$$\text{Cost}_{\text{farm}} = \sum_{k=1}^{n_t} \text{Cost}\left(P_r^k, N^k\right) \times P_r^k \times N^k, \tag{8}$$

where n_t denotes the number of different turbines types used in the wind farm; the parameter N^k represents the number of turbines of type k in the farm that have a rated power P^k. In this case, the total number of turbines (N) in the farm is equal to $\sum_{k=1}^{n_t} N^k$. Subsequently, the COE in $/kWh can be estimated as:

$$\text{COE} = \frac{\text{Cost}_{\text{farm}}}{E_{\text{farm}}} \tag{9}$$

where E_{farm} is the AEP of the farm (as given by Equation 6), expressed in kWh. The above cost functions are estimated using data provided by the Wind and Hydropower Technologies program (US Department of Energy) [20].

3.3. *Wind power density (WPD) estimation*

WPD can be defined as the power available from wind per unit area (perpendicular to the wind direction), averaged over a year at a particular site, and is expressed in watts per square meter. Mathematically, WPD can be defined as:

$$\text{WPD} = \int_{\rho_{\min}}^{\rho^{\max}} \int_{0}^{U^{\max}} \frac{1}{2}\rho U^3 \; p\,(U, \rho)\, dU\, d\rho. \tag{10}$$

The terms and parameters in Equation (10) are the same as those defined in the case of Equation (2). If a parametric wind distribution model is used, the pdf, $p\,(U, \theta, \rho)$, is a well-defined analytical function; in that case, a standard analytical integration may be applicable. However, if a nonparametric wind distribution model is used, numerical integration techniques should be leveraged to estimate the WPD.

For the case studies in this paper, numerical integration has been used to evaluate the WPD from both parametric and nonparametric wind distributions. Similar to the numerical estimation of the AEP, for a set of n_p Monte Carlo sample wind conditions, the approximated WPD is given by:

$$\begin{aligned} \text{WPD} &= \sum_{i=1}^{n_p} \frac{1}{2}\rho^i {U^i}^3 \; p\left(U^i, \rho^i\right) \Delta U\, \Delta\rho, \qquad \text{where} \\ \Delta U\, \Delta\rho &= \left(U_{\max} \times \left(\rho_{\max} - \rho_{\min}\right)\right) / n_p. \end{aligned} \tag{11}$$

For the case studies in this paper, the variation of air density has not been considered. It is also helpful to note that WPD is not a comprehensive measure of the wind resource potential, since it does not account for the variation in wind direction. Owing to the wake effects, the actual power that can be extracted by a wind farm is not proportional to the WPD. The wake effects in turn strongly depend on the wind direction and the farm layout. Further discussion on the limitation of using WPD as a measure of the resource potential can be found in the paper by Zhang et al. [40].

4. Characterizing the uncertainties in wind conditions

For a given farm layout, the AEP is a function of the distribution of wind speed, wind direction, and air density (as shown in Equations 2 and 6). The majority of the wind distribution models are expressed in the form of *parametric* pdfs, as stated in Section 3.1. A smaller set of promising nonparametric wind distribution models have also been recently developed [24].

The ill-predictability of annual wind distribution introduces uncertainties into the predicted probabilities of the sample wind conditions that are used to evaluate the AEP (as in Equation 6). These uncertainties then propagate into the AEP and into the subsequently estimated COE. In this paper, two methods are developed to characterize the uncertainties in wind conditions and to model the propagation of these uncertainties into the farm performance. These methods are: (i) the *parametric wind uncertainty (PWU) model*, and (ii) the *nonparametric wind uncertainty (NPWU) model*. Both methods require multiple-year

data regarding the wind conditions at the concerned site. These two methods are described in the Sections 4.1 and 4.2. Section 4.3 presents and discusses the application of these two uncertainty models to the onshore and offshore case studies introduced earlier in Section 2.

4.1. *Parametric wind uncertainty (PWU) model*

The uncertainty in the *frequency of wind, approaching at a particular speed U, from a particular direction θ, and with an air density ρ*, can be represented in terms of uncertainties in the parameters of the wind distribution. In this case, the distribution parameters are themselves considered to be stochastic over years. The variance of a continuous stochastic parameter provides a standard measure of the uncertainty in that parameter. As illustrated in Section 2.2, the annual distribution of wind conditions varies significantly from year to year. The parametric wind distribution model represented by $p(U, \theta, \rho)$ can therefore be considered a nonlinear function of uncertain distribution parameters. Based on standard uncertainty propagation principles [41], for an m_p-parameter wind distribution model, the corresponding uncertainty can be expressed as:

$$\Sigma_p = J\ \Sigma_q\ J^T, \quad \text{where}$$
$$J = \begin{bmatrix} \frac{\partial p_1}{\partial q_1} & \cdots & \frac{\partial p_1}{\partial q_{m_p}} \\ \vdots & \vdots & \vdots \\ \frac{\partial p_{n_p}}{\partial q_1} & \cdots & \frac{\partial p_{n_p}}{\partial q_{m_p}} \end{bmatrix}. \tag{12}$$

In Equation (12), the covariance matrix Σ_p represents the uncertainty in the *predicted yearly probabilities of the sample wind conditions*; q_k represents the k^{th} parameter of the wind distribution model; the $n_p \times m_p$ covariance matrix for the wind distribution parameters, Σ_q, represents the uncertainty in these parameters; the matrix J represents the Jacobian of the probabilities, with $J_{ik} = \frac{\partial p_i}{\partial q_k}$; and n_p is the number of random sample points used to implement the wind distribution in the estimation of the AEP (Equation 6).

The covariance matrix Σ_q can be determined by fitting a suitable probability distribution to the set of wind distribution parameters estimated for each year over an n-year period. The multivariate normal distribution has been used for this purpose in this paper. The Jacobian matrix J depends on the distribution model that is used to represent the yearly variation in wind conditions. A generic row of the Jacobian matrix for three popular wind distribution models is provided in Table 2. In this paper, the applicability of the PWU method is illustrated by applying it to the case studies in conjunction with the log-normal wind distribution, the Jacobian for which is included in Table 2.

Equation (11) shows that the WPD at a site can be represented as a linear combination of *the predicted yearly probabilities of wind approaching with different sample combinations of wind speed, wind direction, and air density*. Hence, the uncertainty propagating into the WPD, σ_{WPD}, can be modeled as:

$$\sigma^2_{\text{WPD}} = B\ \Sigma_p\ B^T, \quad \text{where}$$
$$B = \begin{bmatrix} B_1 & B_2 & \cdots & B_{n_p} \end{bmatrix}; \quad B_i = \tfrac{1}{2}\rho^i {U^i}^3 \Delta U \Delta\rho. \tag{13}$$

Table 2. Jacobian of the parameters for popular univariate wind distribution models.

Distribution	Distribution pdf	Jacobian
Rayleigh	$p(u) = \frac{u}{\sigma^2} \exp[-x^2 2\sigma^2]$	$J_i = [\frac{p_i}{\sigma}(\frac{u^2}{\sigma^2} - 2)]$
Log-normal	$p(u) = \frac{1}{u\sigma\sqrt{2\pi}} \exp\left[-\frac{(\ln u - \mu)^2}{2\sigma^2}\right]$	$J_i = \left[p_i \frac{\ln u_i - \mu}{\sigma^2}\ ,\ \frac{p_i}{\sigma}\left(\frac{(\ln u - \mu)^2}{\sigma^2} - 1\right)\right]$
Weibull	$p(u) = \frac{k}{\lambda}\left(\frac{u}{\lambda}\right)^{k-1} \exp\left[-\left(\frac{u}{\lambda}\right)^k\right]$	$J_i = \left[p_i\left(\frac{1}{k} + \ln\left(\frac{u}{\lambda}\right) - \left(\frac{u}{\lambda}\right)\ln\left(\frac{u}{\lambda}\right)\right)\ ,\ \frac{kp_i}{\lambda}\left(\left(\frac{u}{\lambda}\right)^k - 1\right)\right]$

Similarly, based on Equation (6), the uncertainty propagating into the AEP, $\sigma_{E_{\text{farm}}}$, can be modeled as:

$$\begin{aligned} &\sigma^2_{E_{\text{farm}}} = C\ \Sigma_p\ C^T, \quad \text{where} \\ &C = \left[C_1\ \ C_2\ \ \cdots\ \ C_{n_p}\right];\quad C_i = 365 \times 24 \times \Delta U \Delta\theta \Delta\rho \times P_{\text{farm}}\left(U^i, \theta^i, \rho^i\right), \end{aligned} \tag{14}$$

where $P_{\text{farm}}(U^i, \theta^i, \rho^i)$ represents the power generated by the farm for a wind coming at speed U^i, from the direction θ^i, and with air density ρ^i; and the term $\Delta U \Delta\theta \Delta\rho$ is representative of the three-dimensional interval size used for the wind condition sampling. Since the capacity factor (CF) of a farm is directly proportional to the AEP, uncertainty in the CF is the same as uncertainty in the AEP of the farm.

The COE of a farm is inversely proportional to the AEP, as given by Equation (9). According to standard uncertainty propagation principles [42], the uncertainty in the COE, σ^2_{COE}, can therefore be represented by:

$$\sigma_{\text{COE}} = \text{COE}\frac{\sigma_{E_{\text{farm}}}}{E_{\text{farm}}}. \tag{15}$$

It is helpful to note that the uncertainty in the wind conditions and the corresponding uncertainties in (i) the AEP and (ii) the COE can also be represented in terms of confidence intervals. Such confidence intervals can be generally determined using maximum likelihood estimation (MLE) techniques.

4.2. *Nonparametric wind uncertainty (NPWU) model*

The nonparametric model provides a more generalized characterization of the uncertainties in wind conditions – not dependent on the type of wind distribution model used to predict the annual variation in wind conditions. In this generalized model, we conceive *the predicted yearly frequency of wind approaching with a particular speed, direction, and air density* to be itself a stochastic parameter; the predicted yearly frequency of a given wind condition can therefore be directly expressed by a probability distribution. Such a distribution readily provides the covariance matrix, Σ^p, that quantifies the uncertainty in the *predicted yearly sample wind probabilities*. The derivation of Σ^p from the uncertainties in the wind distribution parameters, Σ^q, as given by Equation (12), is thereby bypassed.

Figure 7(a) illustrates the frequencies for five sample wind conditions. The details of the five sample wind conditions are provided in Table 3. The wind probability densities (frequencies) for the individual years are represented by the circle symbols. The Y-axis

Table 3. Representative sample wind conditions.

Sample no.	Wind speed (m/s)	Wind direction (degree)	Air density (kg/m^3)
1	6.5	180	1.245
2	9.75	90	1.323
3	3.25	270	1.168
4	4.88	135	1.284
5	11.38	315	1.129

in this figure represents the logarithm of the wind probability densities. The yearly wind frequencies shown in the figure have been normalized through division by the corresponding 10-year wind frequency value for the ease of illustration. The 10-year wind frequency value is represented by the black dashed line. Interestingly, it was found that the *predicted future probability density* (future frequency) of a particular wind condition varies appreciably from year to year over the 10-year period; the oscillations occur over orders of magnitude. Therefore, a second probability distribution can be used to capture the extensive variations in the yearly frequencies of a particular wind condition. Representative Gaussian kernels are used for this purpose, as shown in Figure 7(a). These Gaussian kernels are labeled as *distribution of the probability of sample wind conditions (DPSWC)* in the figure. A more explicit illustration of the use of a representative Gaussian kernel to model the distribution of the yearly frequencies of a sample wind condition is shown in Figure 7(b). It is helpful to note that these Gaussian kernels actually characterize the uncertainties in the yearly wind distributions.

Chowdhury et al. [25] used log-normal distributions to fit the pdfs of *the yearly frequency of each sample wind condition*. In that approach, *the yearly frequencies of sample wind conditions* are considered to be random independent variables. Standard probability distributions were empirically tested. Based on the *coefficient of determination*, R^2, it was found that the log-normal distribution is a reasonably appropriate choice to represent the stochastic nature of the logarithm of the *predicted sample wind probabilities* [25]. However, this choice is dependent on the case studies considered in this paper and the wind distribution model used. The correlation between the frequencies of the individual sample wind conditions is ignored in this approach. The corresponding uncertainty in the AEP was represented by:

$$\sigma^2_{E_{\text{farm}}} = \sum_{i}^{n_p} C_i^2 (p_i \sigma_{\bar{p}_i})^2, \tag{16}$$

where n_p is the number of sample wind conditions, p_i is the predicted yearly frequency of the i^{th} sample wind condition, and $\sigma_{\bar{p}_i}$ represents the uncertainty in the logarithm of the predicted yearly frequency of the i^{th} sample wind condition. The parameter $\sigma_{\bar{p}_i}$ is given by the standard deviation of the log-normal distribution. The cross-covariance terms in the Σ_p matrix are assumed to be zero in this approach. These cross-covariance terms can be precisely defined as $\Sigma_{ij} = E[(p_i - \mu_i)(p_j - \mu_j)],\ i \neq j$, where $E[x]$ represents the expected value of x. For any given wind distribution, the *predicted yearly frequencies of the sample wind conditions* are actually not independent of each other – the corresponding uncertainties are therefore expected to be correlated.

In this paper, we explore the feasibility of accounting for the correlations between the frequencies of the individual sample wind conditions in the NPWU model. A reasonably

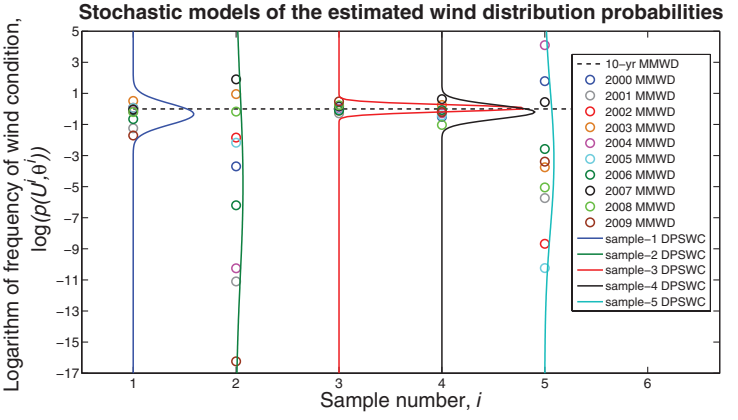

(a) Yearly frequencies of 5 sample wind conditions

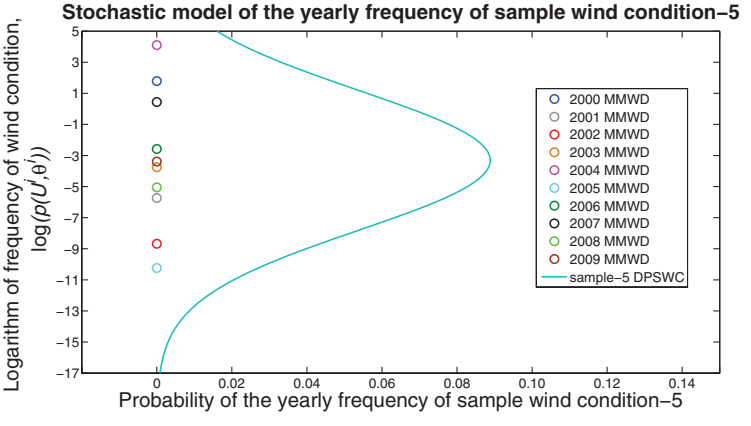

(b) Stochastic model of the yearly frequency of sample wind condition-5

Figure 7. Yearly frequencies of sample wind conditions and their stochastic models.

accurate determination of the AEP of a farm requires a relatively high number (n_p) of sample wind conditions – e.g., a value of $n_p = 100$ is used in this paper when considering the joint variation in wind speed and wind direction. Therefore, to account for the cross-covariance among the yearly frequencies of different sample wind conditions, a 100-dimensional multivariate distribution is required (as opposed to 100 independent univariate distributions). In this case, each dimension corresponds to the yearly frequency of a particular sample wind condition. Therefore, a distribution model that can be readily leveraged for such a high-dimensional multivariate representation is suitable to determine the uncertainty in the *predicted yearly sample wind probabilities*. To this end, a multivariate normal distribution of the logarithm of the *predicted yearly wind probabilities* is used, as given by:

$$p_{\bar{p}} = \frac{1}{(2\pi)^{k/2}\left|\Sigma_{\bar{p}}\right|^{1/2}} \exp[-(\bar{p}-\mu_{\bar{p}})(\Sigma_{\bar{p}})^{-1}(\bar{p}-\mu_{\bar{p}})^{T}], \quad \text{where}$$
$$\bar{p} = [\ln p_1 \quad \ln p_2 \quad \cdots \quad \ln p_{n_p}]. \tag{17}$$

Table 4. Comparison of the attributes of the parametric and the nonparametric wind uncertainty models.

PWU model	NPWU model
Cannot be readily applied to nonparametric wind distribution models	**Can be readily applied to nonparametric wind distribution models**
Requires separate derivation of the Jacobian and determination of the covariance matrix for differing wind distribution models	**Derivation of the Jacobian is not required; provides a generalized uncertainty propagation model**
Less sensitive to the selected set of Monte Carlo sample wind conditions	More sensitive to the selected set of Monte Carlo sample wind conditions
Does not require high-dimensional distribution	Requires fitting a high-dimensional distribution to the frequencies of the sample wind conditions

In Equation (17), $\mu_{\bar{p}}$ and $\Sigma_{\bar{p}}$ are the mean vector and the covariance of the logarithm of the predicted yearly wind probabilities, respectively. The uncertainty in the *predicted yearly sample wind probabilities*, Σ_p, can then be expressed as:

$$\Sigma_p = K\ \Sigma_{\bar{p}}\ K^T, \tag{18}$$

where K is a diagonal matrix such that $K_{ii} = p_i$. The uncertainties in the AEP and in the COE can then be determined using Equations (14) and (15), respectively. Nevertheless, it is helpful to note that the number of wind condition samples used (n_p) is significantly higher than the number of years for which wind data is available. As a result, the estimation of the probability $p_{\bar{p}}$ (from Equation 17) requires fitting a high-dimensional data with a relatively small number of data points. The accuracy of $p_{\bar{p}}$ thus remains a challenging issue, and further research is necessary to resolve this issue.

A comparison of the attributes of the PWU and the NPWU models is provided in Table 4. Positive attributes are represented by bold font in Table 4.

4.3. *Application of the uncertainty models to onshore and offshore sites*

The NPWU model is applied to the 10-year univariate wind speed distributions estimated using the MMWD model. The PWU model is applied to the 10-year univariate wind speed distribution estimated using the log-normal distribution. Zhang et al. [24] have shown that the log-normal distribution and the MMWD compare well for the concerned onshore and offshore sites. The MMWD is however more accurate in both cases [24]. The log-normal distribution comprises two parameters: σ and μ; the corresponding 2×2 parameter-covariance matrix Σ_q is obtained by fitting a multivariate normal distribution to these parameters, estimated for each year from 2000 to 2009.

For the purpose of graphical illustration of the uncertainties, we present the square root of the variances: diagonal terms of the covariance matrix Σ_p from Equation (18). In other words, the uncertainty in the yearly frequency of wind speed U^i and wind direction θ^i is represented by Σ_p^{ii} in the following figures. Figures 8(a) and 8(b) show the uncertainties in the annual univariate wind speed distribution at the onshore and the offshore sites, respectively. The corresponding 10-year wind speed distributions are also presented in this figure. Expectedly, the absolute value of the uncertainty in the *predicted yearly frequency of wind speed* is related to the corresponding *yearly frequency value* (as seen from the overall trend in Figures 8(a) and 8(b)). However, a higher occurrence frequency of a wind

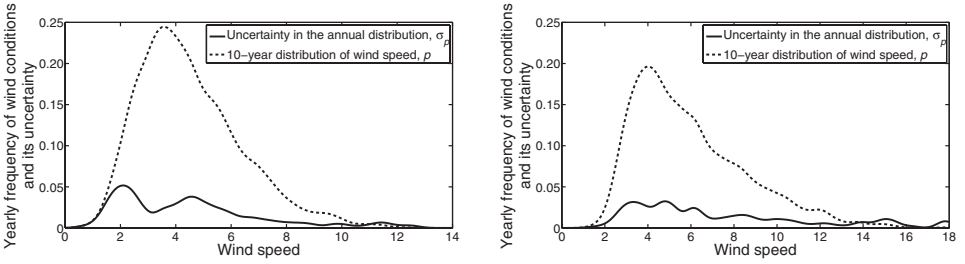

(a) Baker station, ND (onshore) (b) Station 44013, MA (offshore)

Figure 8. Uncertainty in the distribution of wind speed (variance terms in the univariate NPWU model)

speed is not necessarily subject to higher uncertainties – e.g., 3 m/s wind speeds can be simultaneously more frequent (over 10 years) and more reliable (annually, over 10 years) than 2 m/s wind speeds, as seen from Figure 8(a). Hence, oscillations are expected in the variation of uncertainty with respect to wind speed, even though the wind speed distributions are practically unimodal (as seen from Figures 8(a) and 8(b)). In addition, relative to the *predicted yearly frequency values*, the uncertainties are observed to be generally higher for higher wind speeds – approximately, above 10 m/s for the onshore site and above 13 m/s for the offshore site. Overall, it is important to note that for a major portion of the wind distribution (onshore and offshore), the uncertainties are equal to a significant fraction of the corresponding 10-year frequency of wind speed.

Figures 9(a) and 9(b) show the uncertainties in the bivariate annual distribution of wind speed and wind direction at the onshore and offshore sites, respectively. In the case of the bivariate distributions of wind speed and wind direction (Figures 9(a) and 9(b)), the uncertainties seem less related to the magnitude of the corresponding 10-year frequency of wind speed and wind direction (compared with the univariate distribution). For the onshore site, more frequently occurring wind speeds (in the range 2–6 m/s) present higher absolute values of uncertainties, irrespective of the direction from which wind is flowing (Figure 9(a)). At the same time, significant oscillations in the uncertainty are also observed with respect to both wind speed and wind direction, which is expected, as discussed before. On the other hand, in the range of more frequently occurring wind speeds (approximately 3–7 m/s) at the offshore site, the uncertainties are relatively proportional to the corresponding frequency of wind speed and wind direction (as seen from Figures 6(a) and 6(b), and 9(b)). For example, Figure 2(b) shows that 4–6 m/s winds are more frequent from the west direction (270°), and significantly less frequent from the east direction (90°); analogously, Figure 9(b) shows that 4–6 m/s winds flowing from the west direction (270°) are more uncertain than those flowing from the east direction (90°). It can also be observed from Figure 9(b) that higher wind speeds (approximately 12–15 m/s) flowing from the east and north-northwest directions are highly uncertain; these uncertainties are however not likely to affect farm layout planning, since the long-term probability of such high wind speeds is very low. Overall, the visualization of the uncertainties in the predicted yearly wind distributions (as shown in Figures 9(a) and 9(b)) is particularly helpful in conceiving wind farm layouts that would provide reliable performance. *A reliable wind farm design should seek to be minimally sensitive to the more uncertain wind conditions*.

In order to determine the WPD and quantify the uncertainty in the WPD, a set of 100 sample wind conditions are used. The estimated WPDs for the onshore and offshore

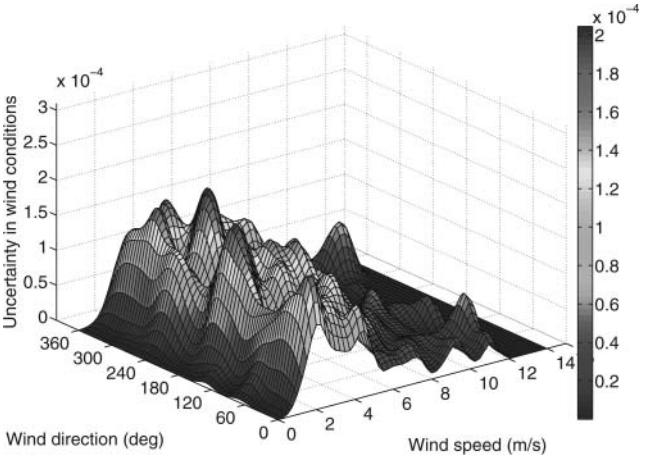

(a) Baker station, ND (onshore)

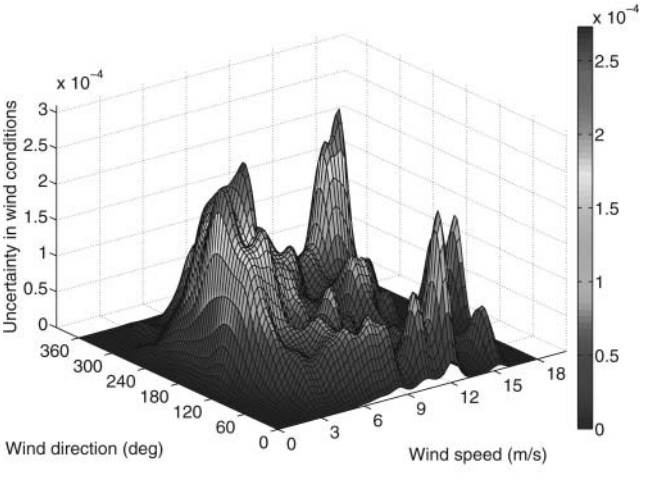

(b) Station 44013, MA (offshore)

Figure 9. Uncertainty in the distribution of wind speed and wind direction (variance terms in the bivariate NPWU model).

sites are summarized in Table 5. The uncertainties in the WPD, estimated using the PWU and NPWU models, are given in Table 6. The first two columns in Table 6 represent the standard deviations (σ) of the estimated individual-year WPDs obtained using the log-normal distribution and the MMWD models. These standard deviations help in validating the PWU and the NPWU models. In Tables 5 and 6, LND represents the log-normal distribution.

It can be seen from Table 5 that the WPDs estimated using the MMWD and the log-normal distributions show reasonable agreement for the onshore and offshore wind sites. Also, in Table 6, the standard deviations of the individual-year WPDs estimated from the two different distributions agree well for the onshore and offshore stations. Table 6 shows that the uncertainty in the WPD, estimated using the PWU model in conjunction with the

Table 5. Estimated 10-year WPDs at the two wind stations.

Site	Using LND (W/m^2)	Using MMWD (W/m^2)
Onshore	93.49	91.97
Offshore	212.83	219.72

log-normal distribution, is reasonably close to the standard deviations of the estimated yearly WPDs. It can also be seen from Table 6 that

- When the cross-covariance terms are ignored, the NPWU model underestimated the uncertainty; and
- When the cross-covariance terms are considered, the NPWU model overestimated the uncertainty.

For the offshore site particularly, the overestimation is substantial. This observation indicates that further research is necessary to develop more accurate determination of the covariance matrix Σ_p for the NPWU model. Nevertheless, if recorded data became available for a greater number of years, the Σ_p matrix in NPWU model can be estimated with better accuracy.

5. Robust wind farm optimization

5.1. *Optimization problem definition*

In this section, we develop and apply a *robust farm optimization* strategy that mitigates the uncertainty in COE, while partially preserving the improvement in COE accomplished through *direct farm optimization*. This robust optimization strategy is applied to design a 25 MW wind farm with given rectangular land dimensions, at the onshore site (refer Section 2). Several different optimization strategies can be defined to address the uncertainties within the scope of maximizing the wind farm performance. In this paper, we apply the following two-step strategy, using the UWFLO method:

- **Step 1:** Apply UWFLO to minimize the COE of the farm.
- **Step 2:** Apply UWFLO to minimize the uncertainty in the COE (σ^2_{COE}). The minimum COE obtained in the previous step is relaxed (increased) by 5% and applied as an additional constraint.

Robust optimization in this case essentially demands searching for Pareto solutions. However, for this paper, we adopt the two-step strategy to investigate what different influences *maximizing farm performance* and *minimizing performance uncertainty* have on layout optimization. For robust wind farm optimization, we consider a bivariate distribution of wind

Table 6. Uncertainty in the predicted yearly WPDs (in W/m^2) at the two stations.

Site	σ of individual-year (LND)	σ of individual-year (MMWD)	σ_{WPD} (PWU)	σ_{WPD} (NPWU, without cross-covariance)	σ_{WPD} (NPWU)
Onshore	11.25	11.90	11.48	3.52	13.54
Offshore	30.10	30.83	31.54	19.23	96.30

Table 7. Specified wind farm properties.

Farm property	Value
Location	Baker, ND (refer Table 1)
Land size (length × breadth)	2800 m × 1200 m
Orientation	North to South lengthwise
Average roughness	0.1 m (grassland)
Density of air	1.2 kg/m^3
Allowed turbines types	GE 1.5 MW and 2.5 MW turbines (6 variations)

speed and wind direction. In Steps 1 and 2, we simultaneously optimize the farm layout and the selection of the turbine type to be installed. This two-step optimization is applied to design a wind farm at the North Dakota location, described in Section 4 and Table 1.

The specified wind farm properties are given in Table 7. The farm is oriented such that the positive X-direction of the layout coordinate system points toward the South. The objective function in Step 1 is normalized by dividing the COE of a candidate farm design by the COE estimated for a reference farm. The reference wind farm comprises 25 "GE 1.5 MW xle" turbines, arranged in a 5 × 5 array layout. The COE of this reference farm ($\mathrm{COE_{ref}}$) was reported to be \$0.023/kWh in the paper on the commercial-scale application of the UWFLO method [14]. Details regarding the features and the compatibility of the "GE 1.5 MW xle" turbine for the concerned site is provided in the same paper [14]. Brief description of the mixed-discrete particle swarm optimization (PSO) algorithm used in the UWFLO method and details of the specified PSO parameters can be found in the paper by Chowdhury et al. [14].

The overall optimization problem for the two steps can be defined as:

$$\begin{aligned}
&\text{Min} \quad f_1(V) = \frac{\mathrm{COE}}{\mathrm{COE_{ref}}} \quad \text{and} \quad f_2(V) = \frac{\sigma_{\mathrm{COE}}}{\mathrm{COE}} \\
&\text{subject to} \\
&\qquad g_1(V) \le 0 \\
&\qquad g_2(V) \le 0 \\
&\qquad g_3(V) \le 0 \\
&\qquad V = \{X_1, X_2, \ldots\ldots, X_N, Y_1, Y_2, \ldots\ldots, Y_N, T_1, T_2, \ldots\ldots, T_N\} \\
&\qquad 0 \le X_i \le X_{\mathrm{farm}} \\
&\qquad 0 \le Y_i \le Y_{\mathrm{farm}} \\
&\qquad T_i \in \{1, 2, \ldots, T^{\max}\},
\end{aligned} \tag{19}$$

where the generic parameters X_i and Y_i represent the location coordinates of the i^{th} turbine; the parameters T_i and $T^{\max}$, respectively, represent the type code of the i^{th} turbine and the total number of turbine types considered (6 in this paper), respectively. Every *commercial turbine type* is integer-coded, going from 1 to 6. In the above problem definition, f_1 and f_2 represent the objective functions minimized in Steps 1 and 2, respectively. Each step thus represents a typical single objective optimization problem. The inequality constraint g_1 represents the minimum clearance required between any two turbines, and is given by:

$$\begin{aligned}
&g_1(V) = \sum_{i=1}^{N} \sum_{\substack{j=1 \\ j \neq i}}^{N} \max\left(\left(D_i + D_j + \triangle_{\min} - d_{ij}\right), 0\right), \quad \text{where} \\
&d_{ij} = \sqrt{\Delta x_{ij}{}^2 + \Delta y_{ij}{}^2}.
\end{aligned} \tag{20}$$

In Equation (20), D_i represents the rotor diameter of turbine i; and $\triangle_{\min}$ is the minimum clearance required between the outer edge of the rotors of the two turbines. In this paper, the value of the minimum spacing between turbines ($\triangle_{\min}$) is set as 10% of the mean rotor diameter (of commercially available turbines) to counter the effects of dynamic loading on turbines. The parameters X_{farm} and Y_{farm} in Equation (19) represent the extent of the rectangular wind farm in the X- and Y-directions, respectively. To ensure the placement of the wind turbines within the fixed-size wind farm, the X_i and Y_i bounds are reformulated into an inequality constraint, $g_2(V) \leq 0$. The constraint g_2 is expressed by:

$$g_2(V) = \frac{1}{2N}\left(\begin{array}{l}\dfrac{1}{X_{\text{farm}}}\displaystyle\sum_{i=1}^{N}\max\left(-X_i, X_i - X_{\text{farm}}, 0\right) \\ +\dfrac{1}{Y_{\text{farm}}}\displaystyle\sum_{i=1}^{N}\max\left(-Y_i, Y_i - Y_{\text{farm}}, 0\right)\end{array}\right).$$

The constraint g_3 is the COE constraint that is applied only in Step 2. This constraint is defined as:

$$g_3(V) = \text{COE} - 1.05 \times \text{COE}_{\min}, \tag{21}$$

where $\text{COE}_{\min}$ is the minimum COE obtained through optimization in Step 1.

5.2. *Results and discussion*

For the optimization Steps 1 and 2, we allow 100,000 evaluations (each) of the energy production model. The convergence histories of the two optimizations are shown in Figures 10(a) and 10(b). The minimum COE obtained in Step 1 is 0.0185/kWh. The same turbine was selected as the optimal type in Steps 1 and 2 – the GE 2.5 MW xl with a 100 m tower and a 100 m rotor diameter. The optimized farm layouts obtained in Steps 1 and 2 are shown in Figures 11(a) and 11(b), respectively. Details of the farm performances and of the corresponding uncertainties obtained in the two steps are summarized in Table 8. The last

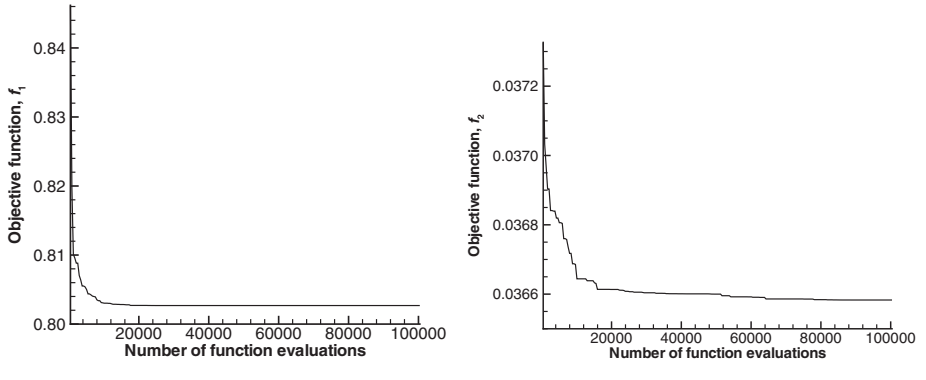

(a) Step-1: Minimizing the COE

(b) Step-2: Minimizing the uncertainty in the COE

Figure 10. Convergence histories of the mixed-discrete PSO.

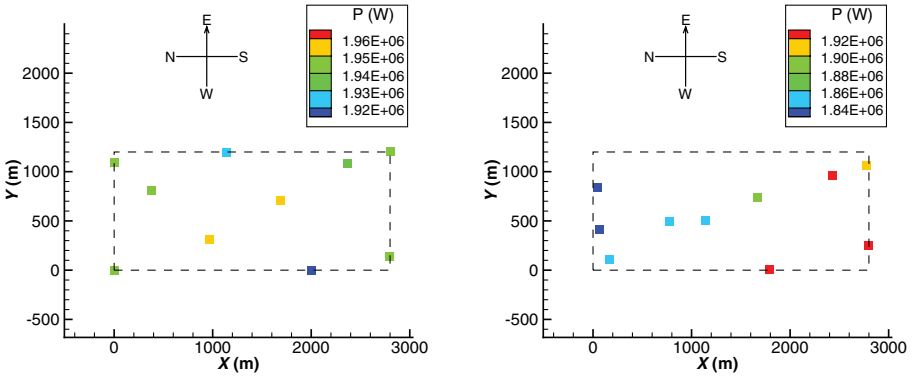

(a) Step-1: Minimizing the COE

(b)Step-2: Minimizing the uncertainty in the COE

Figure 11. Optimized wind farm layouts.

column in this table represents the percentage change in values from Step 1 to Step 2, i.e., 100×(Step 2 – Step 1)/Step 1.

We observe from Figures 10(a) and 10(b) that the *minimization of the COE* converges faster than the *minimization of the uncertainty in the COE*. In the latter case, the UWFLO method seeks to simultaneously (i) accomplish a COE less than 105% of the minimum COE obtained in Step 1, and (ii) minimize the overall uncertainty in the COE. Intuitively, the *minimization of the uncertainty in the COE* should seek to reduce the *sensitivity of the* "AEP" to the "relatively more uncertain wind conditions". The reduction in wake losses through layout optimization is thus expected to be biased toward wind speeds and wind directions that present relatively lower uncertainties. On the other hand, the minimization of the COE seeks to increase the overall power generation from the entire range of wind conditions. Expectedly, robust wind farm optimization presents conflicting objectives.

Table 8 shows that the reduction in farm performance in Step 2 (compared with Step 1) is within acceptable limits. More importantly, it can be observed from Table 8 that the uncertainty in farm performance decreases by approximately 3% in Step 2. Such a significant mitigation of wind resource uncertainties without unreasonably compromising on the farm performance is uniquely helpful to wind project planning. Future research in "robust optimization of wind farms" should explore a more typical multiobjective optimization scenario to simultaneously maximize the farm performance and minimize the performance uncertainty. The distinct natures of the two optimization steps are also illustrated by the optimized layouts shown in Figures 11(a) and 11(b). We observe that the minimization of the COE has produced a layout that is well spread in all directions. This resulting layout pattern can be

Table 8. Attributes of the optimized wind farms.

Parameter	Step 1	Step 2	Change
Capacity factor (CF)	0.776	0.752	3.2% decrease
Percentage uncertainty in CF	3.7%	3.6%	2.7% decrease
COE ($/kWh)	0.0185	0.0191	3.2% increase
Percentage uncertainty in COE ($f_2 \times 100$)	3.7%	3.6%	2.7% decrease

attributed to the nature of the wind distribution at this site – the more frequently occurring wind speeds of approximately 2–5 m/s come from all directions except the Northeast. On the other hand, the minimization of the uncertainty in the COE has produced a layout that is relatively more well spread in the North-South direction. A comprehensive investigation of the sensitivity of the optimized layouts to the uncertainties in wind conditions should provide further insights into the crucial aspects of robust wind farm design.

It can be seen from Table 8 that the relative uncertainties in the AEP and the COE of the optimized farms are approximately 4%. Considering that *the NPWU model without the cross-covariance terms* underestimated the uncertainties, the actual uncertainties in the AEP and the COE could be higher. Such uncertainties could exert an appreciable influence on the economic feasibility of a wind farm. Hence, an accurate quantification and due consideration of these uncertainties are of primary importance when conceiving a wind energy project.

6. Conclusion

Efficient planning of a wind energy project demands appropriate consideration of the factors that influence the farm performance, several of which are highly uncertain. The ill-predictability of wind conditions is one of the primary sources of such uncertainties. This paper presents a new methodology (i) to characterize the *uncertainties in the predicted yearly wind distribution*, and (ii) to model the propagation of these uncertainties into the overall farm performance evaluation. Illustrations of the annual wind distributions over the 10-year period (2000–2009) show that significant year-to-year variations exist at the studied onshore and offshore sites. Two uncertainty models are developed to capture these variations: a parametric model that can be implemented in conjunction with a wide variety of parametric wind distribution models, and a nonparametric model that can be implemented with both parametric and nonparametric wind distribution models. The parametric model is developed based on standard uncertainty propagation principles, and the pertinent propagation functions are derived for the one-dimensional Weibull, log-normal, and Rayleigh distributions. In the nonparametric model, the annual frequency of occurrence of a particular wind condition is itself treated as a stochastic parameter, and is represented by a multivariate normal distribution. Although the nonparametric model is more universally applicable, its accuracy may be limited since a small data set is available to estimate a high-dimensional multivariate stochastic model. Further advancement of the nonparametric model is necessary to avoid this limitation. Expectedly, the parametric model was found to provide a more accurate estimation of the uncertainty in the predicted WPD for the studied sites. It is observed that the uncertainties in the predicted yearly wind frequencies are approximately 10–20% at the onshore and offshore sites. The case studies showed that the uncertainties in wind conditions are not necessarily proportional to the predicted yearly frequency of wind conditions. Therefore, when conceiving wind farm designs, it is important to understand which range(s) of wind conditions (speed and direction) is both frequent (over the long term) and reliable (from year to year). Robust farm layout design should therefore ensure greater dependence on wind conditions that present the best combination of the following two attributes: (i) higher *long-term probability* and (ii) higher *year-to-year reliability*.

The incorporation of the uncertainty propagation models into the UWFLO framework provided the foundation for *robust wind farm optimization*. The new robust UWFLO framework is applied to design a 25 MW onshore wind farm that is both high-performing and reliable. The *minimization of the COE* and the *minimization of the uncertainty in the COE*

produced characteristically different farms layouts. Typical multiobjective optimization should provide more helpful insights into the nature of the tradeoffs between these two objectives. Overall, the case studies established that appropriate estimation and consideration of the long-term wind uncertainties are crucial for both wind resource assessment and wind farm layout optimization. Future research in this direction should also investigate the interaction of "the uncertainties occurring due to year-to-year variations" and "the uncertainties introduced by the MCP methods used in commercial wind resource assessment."

Acknowledgements

Support from the National Science Foundation Awards CMMI-1100948 and CMMI-0946765 is gratefully acknowledged.

References

[1] WWEA, *World wind energy report 2010*, WWEA, Bonn, Germany, 2011.
[2] ODOE, Oregon Department of Energy (ODOE): Renewable energy – Wind Resource Assessment (n.d.). Available at http://www.oregon.gov/ENERGY/RENEW/Wind/Assessment.shtml.
[3] EWEA, Wind energy – the facts (n.d.). Available at http://www.ewea.org/index.php?id=91.
[4] P. Sorensen and T. Nielsen, *Recalibrating wind turbine wake model parameters – validating the wake model performance for large offshore wind farms*, European Wind Energy Conference and Exhibition, February, Athens, Greece, 2006.
[5] N.O. Jensen, *A note on wind turbine interaction*, Report no. M-2411, Risoe National Laboratory, Roskilde, Denmark, 1983.
[6] I. Katic, J. Hojstrup, and N.O. Jensen, *A simple model for cluster efficiency*, European Wind Energy Conference and Exhibition, Rome, Italy, 1986.
[7] R. Mikkelsen, J.N. Sørensen, S. Øye, and N. Troldborg, *Analysis of power enhancement for a row of wind turbines using the actuator line technique*, J. Phys.: Con. Series 75 (2007), p. 012044.
[8] H.G. Beyer, B. Lange, and H.P. Waldl, *Modelling tools for wind farm upgrading*, European Union Wind Energy Conference, May, Goborg, Sweden, 1996.
[9] S.A. Grady, M.Y. Hussaini, and M.M. Abdullah, *Placement of wind turbines using genetic algorithms*, Renew. Energ. 30 (2005), pp. 259–270.
[10] S. Sisbot, O. Turgut, M. Tunc, and U. Camdali, *Optimal positioning of wind turbines on Gökçeada using multi-objective genetic algorithm*, Wind Energ. 13 (2009), pp. 297–306.
[11] J.S. Gonzleza, A.G.G. Rodriguezb, J.C. Morac, J.R. Santos, and M.B. Payan, *Optimization of wind farm turbines layout using an evolutive algorithm*, Renew. Energ. 35 (2010), pp. 1671–1681.
[12] L. Chen and E. MacDonald, *A new model for wind farm layout optimization with landowner decisions*, ASME 2011 International Design Engineering Technical Conferences & Computers and Information in Engineering Conference, August, Washington, DC, 2011.
[13] S. Chowdhury, J. Zhang, A. Messac, and L. Castillo, *Unrestricted wind farm layout optimization (UWFLO): investigating key factors influencing the maximum power generation*, Renew. Energ. 38 (2012), pp. 16–30.
[14] S. Chowdhury, J. Zhang, A. Messac, and L. Castillo, *Developing a flexible platform for optimal engineering design of commercial wind farms*, ASME 2011 5th International Conference on Energy Sustainability & 9th Fuel Cell Science, Engineering and Technology Conference, August, Washington, DC, 2011.
[15] S. Frandsen, R. Barthelmie, S. Pryor, O. Rathmann, S. Larsen, J. Hojstrup, and M. Thogersen, *Analytical modeling of wind speed deficit in large offshore wind farms*, Wind Energ. 9 (2006), pp. 39–53.
[16] R.B. Cal, J. Lebron, H.S. Kang, C. Meneveau, and L. Castillo, *Experimental study of the horizontally averaged flow structure in a model wind-turbine array boundary layer*, J. Renew. Sustainable Energ. 2 (2010), pp. 013106–013131.
[17] C. Kiranoudis, N. Voros, and Z. Maroulis, *Shortcut design of wind farms*, Energ. Policy 29 (2001), pp. 567–578.

[18] J.K. Kaldellis and T.J. Gavras, *The economic viability of commercial wind plants in Greece: a complete sensitivity analysis*, Energ. Policy 28 (2000), pp. 509–517.
[19] S. Herman, *Probabilistic cost model for analysis of offshore wind energy costs and potential*, Report no. ECN-I-02-007, Energy Research Center of the Netherlands, Petten, The Netherlands, 1983.
[20] NREL, *Jobs and economic development impact (JEDI) model*, NREL, Golden, CO, 2009.
[21] T.T. Cockerill, *Jobs and economic development impact (JEDI) Model*, Report no. JOR3-CT95-0087, Renewable Energy Centre, University of Sunderland, Sunderland, UK, 1997.
[22] J. Carta, P. Ramírez, and S. Velázquez, *A review of wind speed probability distributions used in wind energy analysis case studies in the canary islands*, Renew. Sustain. Energ. Rev. 13 (2009), pp. 933–955.
[23] E. Morgan, M. Lackner, R. Vogel, and L. Baise, *Probability distributions for offshore wind speeds*, Energ. Conv. Manag. 52 (2011), pp. 15–26.
[24] J. Zhang, S. Chowdhury, A. Messac, and L. Castillo, *Multivariate and multimodal wind distribution model based on kernel density estimation*, ASME 2011 5th International Conference on Energy Sustainability & 9th Fuel Cell Science, Engineering and Technology Conference, August, Washington, DC, 2011.
[25] S. Chowdhury, J. Zhang, A. Messac, and L. Castillo, *Characterizing the uncertainty propagation from the wind conditions to the optimal farm performance*, 52nd AIAA/ASME/ASCE/AHS/ASC Structures, Structural Dynamics, and Materials Conference, AIAA 2011-1821, April, Denver, CO, 2011.
[26] NDSU, North Dakota Agricultural Weather Network (NDAWN) (n.d.). Available at http://ndawn.ndsu.nodak.edu/.
[27] NOAA, National Data Buoy Center (NDBC) (n.d.). Available at http://www.ndbc.noaa.gov/.
[28] T. Burton, S. David, N. Jenkins, and B. Ervin, *Wind Energy Handbook*, John Wiley & Sons, New York, 2001.
[29] M.A. Lackner and C.N. Elkinton, *An analytical framework for offshore wind farm layout optimization*, Wind Eng. 31 (2007), pp. 17–31.
[30] R.E. Vega and C.W. Letchford, *Wind directionality and the estimate of wind energy: the case for West Texas*, 2008 Annual Conference – The Academy of Medicine, Engineering and Science of Texas, March, College Station, TX, 2008.
[31] J. Carta, P. Ramírez, and S. Velázquez, *A review of wind speed probability distributions used in wind energy analysis case studies in the canary islands*, Renew. Sustain. Energ. Rev. 13 (2009), pp. 933–955.
[32] E. Erdem and J. Shi, *Comparison of bivariate distribution construction approaches for analysing wind speed and direction data*, Wind Energ. 14 (2011), pp. 27–41.
[33] J. Simonoff, *Smoothing Methods in Statistics*, Springer, New York, 1996.
[34] V. Epanechnikov, *Non-parametric estimation of a multivariate probability density*, Theor. Probab. Appl. 14 (1969), pp. 153–158.
[35] T. Duong and M. Hazelton, *Plug-in bandwidth matrices for bivariate kernel density estimation*, Nonparametr. Stat. 15 (2003), pp. 17–30.
[36] C.J.R. Sheppard, *Analysis of the measure-correlate-predict methodology for wind resource assessment*, Master's thesis, Humbolt State University, Arcata, CA, 2009.
[37] A. Kusiak and H. Zheng, *Optimization of wind turbine energy and power factor with an evolutionary computation algorithm*, Renew. Energ. 35 (2010), pp. 1324–1332.
[38] M. Sobol, *Uniformly distributed sequences with an additional uniform property*, USSR Comp. Math. Math. Phys. 16 (1976), pp. 236–242.
[39] A.A. Mullur and A. Messac, *Extended radial basis functions: more flexible and effective metamodeling*, AIAA J. 43 (2005), pp. 1306–1315.
[40] J. Zhang, S. Chowdhury, A. Messac, and L. Castillo, *A comprehensive measure of the energy resource potential of a wind farm site*, ASME 2011 5th International Conference on Energy Sustainability & 9th Fuel Cell Science, Engineering and Technology Conference, August, Washington, DC, 2011.
[41] B. Ochoa and S. Belongie, *Covariance Propagation for Guided Matching*, University of California, San Diego, La Jolla, CA, 2008.
[42] V. Lindberg, *Vern Lindberg's Guide to Uncertainties and Error Propagation*, Rochester Institute of Technology, Rochester, NY, 1999.